Journal of Applied Electrochemistry (2006) 36:973–981
DOI 10.1007/s10800-006-9124-0

An electrochemical and *in situ* SERS study of Cu electrodeposition from acidic sulphate solutions in the presence of 3-diethylamino-7-(4-dimethylaminophenylazo)-5-phenylphenazinium chloride (Janus Green B)

B. BOZZINI*, C. MELE, L. D'URZO and V. ROMANELLO
Dipartimento di Ingegneria dell'Innovazione, Università di Lecce, via Monteroni, I-73100, Lecce, Italy
*(*author for correspondence E-mail: benedetto.bozzini@unile.it)*

Received 20 June 2005; accepted in revised form 16 January 2006

Key words: copper, electrodeposition, JGB, SERS, ULSI fabrication

Abstract

This paper deals with the behaviour of 3-diethylamino-7-(4-dimethylaminophenylazo)-5-phenylphenazinium chloride (Janus Green B, JGB) during Cu electrodeposition from an acidic sulphate solution. This investigation was carried out by cyclic voltammetry and *in situ* Surface Enhanced Raman spectroelectrochemistry. Parameters describing nucleation, charge-transfer kinetics, mass-transport effects and anodic stripping behaviour were derived by quantitative analysis of the cyclic voltammograms. JGB effects have been found on nucleation rate, exchange current density and cathodic Tafel slopes. Voltammetry highlighted the cathodic reactivity of JGB. *In situ* SERS spectra were measured under both cathodic and anodic polarisation, in the range 0.2–0.7 V vs Ag/AgCl. SERS spectra were recorded also in the galvanostatic mode. SERS effect variations with potential and potentiostatic polarisation time were studied.

1. Introduction

The widely-investigated processes of Cu electrodeposition for ultra large scale of integration (ULSI) fabrication rely heavily on the use of complex blends of organics commonly categorised as: (i) carriers, (ii) brighteners or accelerators and (iii) levellers. Carriers and levellers are sometimes denominated suppressors, implying the fact that they enhance electrodeposition overvoltage. Typically: (i) carriers are polyethylene glycols (PEG), (ii) brighteners are molecules with thiol RSH and disulfide RSSR bonds and sulfonic acid groups (i.e.: Bis-(3-sulfopropyl)-disulfide, SPS) and (iii) levellers are molecules with amine functionality or aromatic rings.

3-Diethylamino-7-(4-dimethylaminophenylazo)-5-phenylphenazinium chloride, also denominated Janus Green B (JGB) has been studied in some publications dealing with via filling and superfilling, in conjunction with other additives: Cl^-, PEG and SPS [1–6]; thiourea has been added to the 4-additive chemistry in [7]. Addition of JGB only to the acidic sulphate Cu bath was shown not to produce levelling, but to yield conformal deposition [1], while the synergy between JGB and SPS seems to be vital for successful levelling [2].

Thus, only a limited amount of electrochemical information on the specific action of JGB is available. The potentiodynamic behaviour of the systems containing just Cl^- and PEG or these two additives together with JGB [6] or both JGB and SPS [1] has been reported not to differ quantitatively; JGB thus sort of quenches the accelerating effect of SPS. The inhibiting effect of JGB seems to be more effective at higher RDE rotation rates, suggesting that the cathodic inhibition is controlled by mass transport [1, 3, 6, 7].

As far as the properties of the Cu electrodeposits are concerned, FESEM investigations on patterned electrodes have shown that, in the presence of JGB, PEG particles are excluded from the vias [3, 6]. A grain-refining effect of JGB in conjunction with SPS has been reported in Cl^- –PEG systems [1, 3]. In the presence of Cl^-, PEG, SPS and JGB, TEM micrographs are characterised by two kinds of morphology: one with flake-like crystallites and another one exhibiting no defined texture; JGB suppresses the tendency to form twins introduced by the addition of SPS to the Cl^-–PEG bath [1]. GDOES analyses of Cu layers deposited from the bath containing Cl^-, PEG, SPS, JGB and thiourea showed that elements from the additives (C, H and S) could be found only in the topmost layers of the electrodeposits [7].

Several electrochemical methods and *ex situ* analytical techniques have been used in order to differentiate the effects of the relevant organic species, but *in situ* spectroelectrochemistry has received limited attention. Apart from previous work in our group [8–10], the

authors are aware of few papers dealing with SERS during the electrodeposition of Cu both in the absence [11] and in the presence of organic additives [12].

In this work, we focus on the effects of JGB on the Cu electrodeposition process in the absence of other additives. We report electrochemical (cyclic voltammetry with a rotating disk electrode) and spectroelectrochemical (*in situ* surface-enhanced Raman spectroscopy (SERS)) results on the effects of JGB during the electrodeposition of Cu from a conventional acidic sulphate electrolyte.

2. Experimental

The electrodeposition baths were: $CuSO_4{\cdot}5H_2O$ 20 mM, H_2SO_4 0.5 M. To this solution JGB (Aldrich) 1 mg l^{-1} was added. The structural formula of JGB is reported in Figure 1. JGB was dissolved in ultrapure water to make a 0.1 g l^{-1} stock solution, aliquots of the stock solution were added to the plating bath. We used analytical grade chemicals and ultra-pure water with a resistivity of 18.5 MΨ cm from a Millipore-Milli-Q system. The solutions were degassed by N_2 bubbling and maintaining the solution under a N_2 blanket during the measurements. In order to minimise organic contamination all the items in contact with the working electrolyte were rinsed with concentrated HNO_3 before and after each experiment and stored in 20 vol % HNO_3 diluted with ultra-pure water.

Electrochemical measurements were performed with an AMEL 5000 programmable potentiostat and a three-electrode cylindrical cell. A PAR Model 636 rotating-disk electrode (RDE) was used. The working electrode (WE) was a PAR Pt rotating disk of 4 mm diameter. The counter electrode (CE) was a platinised Ti mesh electrode 10 cm^2 in area. The reference electrode (RE) was an AMEL Ag/AgCl containing a 3 M KCl separated from the electroplating solution by a porous ceramic insert. The RE tip was placed at a distance of 5 mm from the WE rim. Ohmic corrections applied by the positive feedback method were considered, but proved irrelevant due to the high conductivity of the solution. Voltages are reported against Ag/AgCl.

SERS measurements were performed with a LabRam confocal Raman system. Excitation at 633 nm was provided by a He–Ne laser, delivering 7 mW at the sample surface. A 50× long-working-distance objective was used. *In situ* spectroelectrochemistry was carried out in a cell with a vertical polycrystalline Cu disc WE of diameter 5 mm embedded in a Teflon cylindrical holder. A metallographic polishing procedure, consisting of wet grinding with 2400 grit SiC paper, allowed excellent reproducibility. The CE was a Pt wire loop (1.25 cm^2) concentric and coplanar with the WE disc. The RE was placed in a separate compartment. The RE probe tip was placed 3 mm from the rim of the working electrode disc. Raman intensities are normalised over the acquisition time – so that the intensities can be compared – and proportional to the discharge current of the CCD element corresponding to a given Raman shift, uncorrected for quantum efficiency. Acquisition times of SERS spectra were: 7 s in the range from −0.1 to −0.4 V; 30 s from −0.5 to −0.8 V; and 5 s from 0.1 ÷ 0.4 V, respectively.

3. Results and discussion

3.1. *Cyclic voltammetry*

CV curves for the additive-free and for the JGB-containing baths are shown in Figure 2. The CVs were measured with a scan rate of 10 mV s^{-1} in the potential range: +0.75 to −0.75 V. Two subsequent CVs were recorded. Each set of experiments carried out by sequentially changing the rotation rate, was replicated thrice. The cycles started and finished at the most anodic potential in order to gain information on the nucleation behaviour during the forward, cathodic-going scan. The initial conditions of the Pt electrode were restored by dissolving residual Cu in concentrated HNO_3 before measuring each voltammogram; notwithstanding this caution, no appreciable differences were noticed between the first and the second scans recorded sequentially and the electrochemical stripping gave rise to a starting surface that essentially behaves like the chemically stripped one.

The curves reported in Figure 2 exhibit the same qualitative features, apart from the fact that the presence of JGB correlates with: (i) higher terminal cathodic c.d.s and (ii) a more marked nucleation loop. Inspection of the cathodic going scan of the CV curves shows a

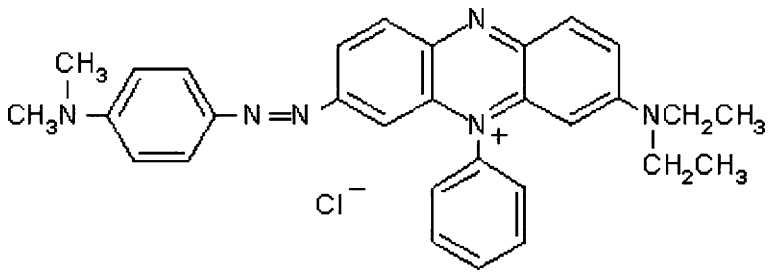

Fig. 1. Structrural formula of 3-diethylamino-7-(4-dimethylaminophenylazo)-5-phenylphenazinium chloride (Janus Green B, JGB).

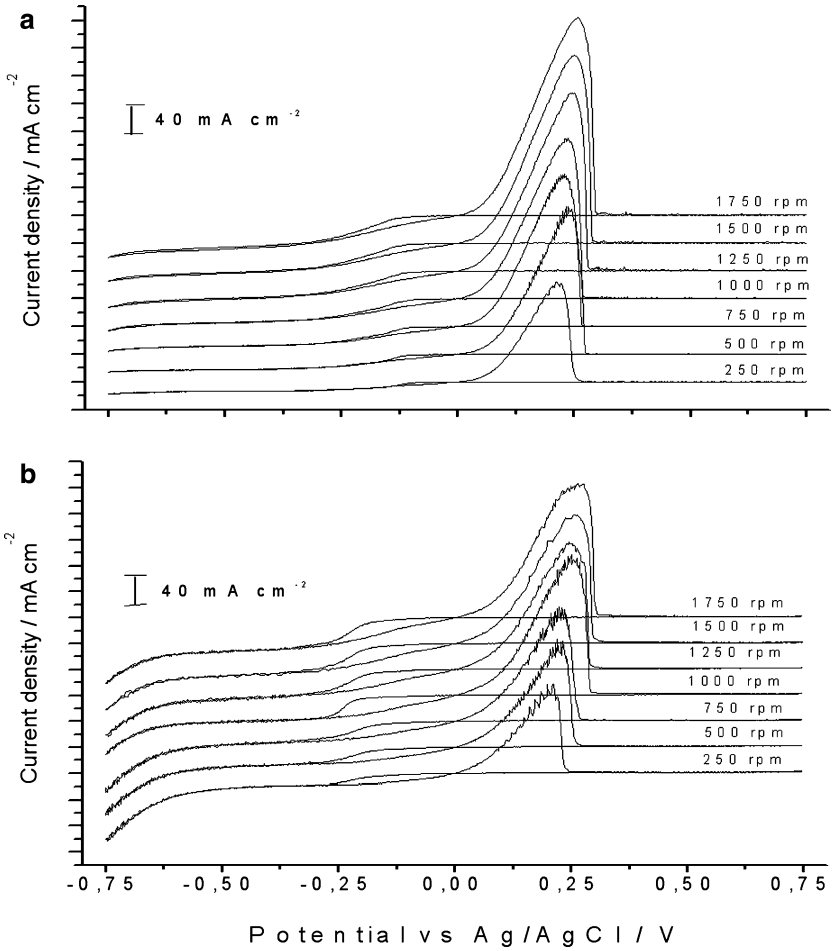

Fig. 2. Cyclic voltammetry of the (a) additive-free and (b) JGB-containing acidic Cu eletrodeposition bath, as a function of the RDE rotation rate. Scan rate: 10 mV s^{-1}.

Tafel-type growth followed by a limiting current density (c.d.). At more cathodic potentials, a second Tafel-type growth starts, corresponding to the onset of hydrogen evolution and JGB reaction. The Cu nucleation and growth behaviour, giving rise to the details of the cathodic portions of the curves, differ in a statistically significant way in the absence and in the presence of JGB. The anodic going scan crosses the forwards scan giving rise to a nucleation loop and eventually an anodic stripping peak is observed.

We carried out a quantitative analysis of the CVs addressing the following points: (i) the nucleation behaviour on a Pt electrode; (ii) the Cu-electrodeposition kinetics at Cu-covered electrodes, including mass-transport contributions; (iii) quantification of the anodic stripping peaks, incorporating information concerning both Cu deposition efficiency and peculiarities of the Cu corrosion process in the relevant environments.

3.1.1. *Nucleation of Cu at a polycrystalline Pt electodes*
Details of the data treatment procedure can be found in a companion paper [10]. The following parameters were extracted from the nucleation portion of the CVs: the nucleation potential V_N and the width ΔV_N of the c.d. transition corresponding to nucleation. Owing to the cathodic reactivity of JGB (obvious Tafel-type growth) the limiting c.d. interval is restricted and V_N and ΔV_N have been evaluated by NLLS fitting for cathodic potentials between −0.050 and −0.45 V.

Figure 3 shows the dependence of V_N and ΔV_N on rotation rate and bath chemistry. Figure 3a shows: (i) a tendential cathodic shift of V_N on increasing the rotation rate and (ii) more cathodic values in the presence of JGB. This can be related to the fact that JGB has been reported to exhibit mass-transport controlled levelling effectiveness [1, 3, 6, 7]. The fact that the nucleation potential is displaced to more cathodic values in the presence of JGB can be related to the adsorption of this substance at the growing electrode. Figure 3b shows that systematically narrower transitions are found in the presence of JGB, denoting a higher nucleation rate. As far as mass-transport effects on ΔV_N are concerned, this quantity is found to grow in the absence of JGB and to be essentially constant in its presence, coherently with the behaviour of V_N.

3.1.2. *Cu electrodeposition kinetics*
The cathodic portion of the anodic-going scans was analysed numerically with a Butler–Volmer model and allowance for a limiting c.d. [13]. The parameters

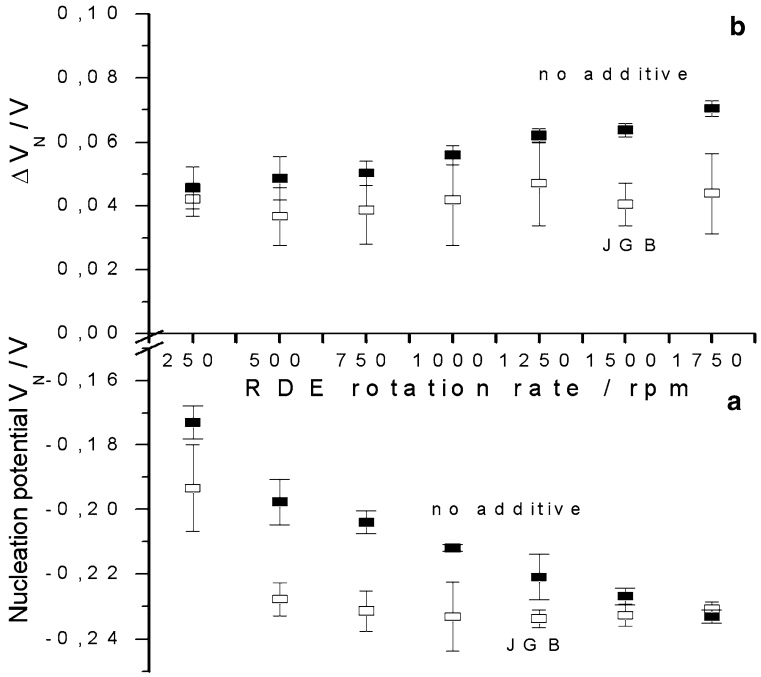

Fig. 3. (a) Half-wave potential V_N and (b) width ΔV_N of the nucleation voltammetric transition as a function of RDE rotation rate and bath chemistry.

obtained by non-linear least-squares (NLLS) fitting were the exchange c.d. i_o, the cathodic Tafel slope β_C, the limiting c.d. i_L and the open-circuit potential V_o. The average parameter estimates and their standard deviations are evaluated from the three replicated runs. i_L is reported as a function of the RDE rotation rate in Figure 4. It should be noted that the 95% confidence intervals estimated by NLLS are always smaller than the standard deviation of the parameter estimates computed from the three replicates. A constant value of 0.120 V dec^{-1}, commonly found in the literature, was set as fixed for the anodic Tafel slopes because we intended to concentrate on the cathodic range.

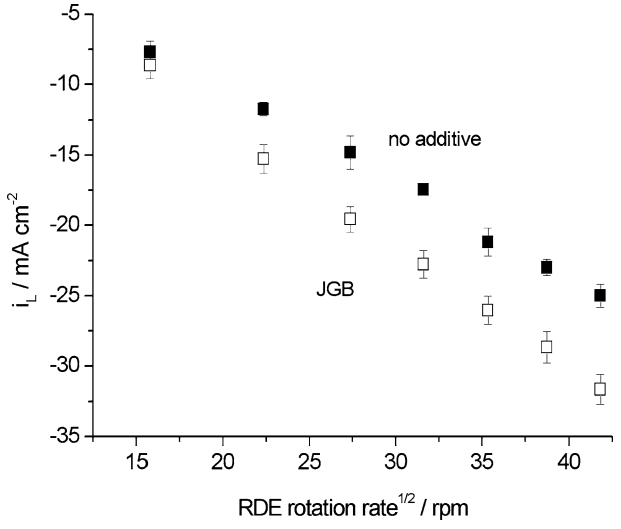

Fig. 4. Limiting current density i_L NLLS estimates as a function of the square root of RDE rotation rate and bath chemistry.

No appreciable dependence of V_o on rotation rate for both baths can be observed, as expected. Upon averaging across the rotation rates, the additive-free bath exhibits $V_o = -0.018 \pm 0.002$ V and the JGB-containing one 0.010 ± 0.001 V. This ennobling effect can be related to the adsorption of the cationic organic species.

The exchange current density is not affected by the mass-transport conditions. The trend of the i_o expectations with rotation rate for the additive-free solution is not statistically significant owing to the estimated values of the standard deviations. We therefore pooled all the i_o values and their standard deviations and averaged across the rotation rates. One thus finds i_o values of 2.62 ± 0.48 and 6.02 ± 0.37 mA cm^{-2} in the absence and presence of JGB, respectively. Values close to 2 mA cm^{-2} have been reported for the additive-free bath [14, 15] and 0.5 mA cm^{-2} was found when SPS, PEG and Cl^- are simultaneously present [16]. The detailed balance close to equilibrium is thus shifted to more active conditions in the presence of JGB. A similar effect has been found with PEG [8] and SPS [10] and might be related to the formation of mixed complexes; the β_C values found in this research (see below) support this view.

Again, in the statistical sense given above, no dependence of β_C on the RDE rotation rate was found. By averaging across the rotation rates, we found cathodic Tafel slopes of 0.119 ± 0.003 and 0.090 ± 0.008 V dec^{-1} for baths without and with JGB. Typical literature values for the additive-free bath lie close to 0.120 V dec^{-1} [16, 17], both in the presence and absence of Cl^-. No appreciable variations were found when SPS was used together with PEG and Cl^- [16]. β_C values

close to 0.120 V dec^{-1} are customarily regarded as corresponding to an EE mechanism going through Cu^+ with reduction of the intermediate being the rds; values close to 0.090 V dec^{-1}, such as that found in this study in the presence of JGB, are interpreted considering that chemical reduction of a Cu(I)-containing intermediate occurs [17].

Figure 4 reports the Levich plots for baths without and with JGB. Fitting of data for the two baths with a line with zero intercept yields estimates of the diffusion coefficient D; the following result were obtained: (i) in the additive-free solution $(4.24 \pm 0.55) \times 10^{-6}$ cm^2 s^{-1}, linear correlation coefficient $\rho^2 = 0.9903$; in the presence of JGB $(6.76 \pm 0.85) \times 10^{-6}$ cm^2 s^{-1}, linear correlation coefficient $\rho^2 = 0.9905$. The kinematic viscosity of pure water was used in the relevant computations.

The addition of JGB causes an increase in the effective diffusion coefficient of Cu^{2+}, similar effects have been reported for organic species in acidic sulphate Cu electrodeposition baths [8, 14].

Figure 2 shows that higher cathodic terminal c.d.s are found in the presence of JGB. This fact can be related to the cathodic activity of JGB. In order to compare the cathodic behaviour in the presence and absence of JGB, in Figure 5 we report the ratio of the charges consumed during the cathodic portions of the scans (i.e. the sum of the cathodic charges consumed during both the forward and backward scans) in JGB-containing and additive-free baths, as a function of rotation rate. A decreasing trend is found, with values higher than 1: enhanced mass transport at the cathode–electrolyte interface depresses the contribution of JGB to the total c.d., suggesting a mass-transport controlled competition between the reduction of Cu^{2+} and JGB.

3.1.3. *Voltammetric anodic stripping*

The analysis of the voltammetric stripping peaks has been proposed as an approach yielding integral information on bath chemistry. Commonly, the ratio of the areas of the anodic stripping peaks in the absence and presence of selected additives is adopted as an indication of the acceleration or inhibition of the electrodeposition process, brought about by relevant changes in bath chemistry; this method is commonly denominated cyclic voltammetric stripping (CVS) [5, 18]. In the present investigation we extracted two quantities from the anodic stripping peaks: (i) the integrated charge under the peak A_A and (ii) the potential at which the half maximum of the peak $V_{N1/2}$ is found. The physical meaning of the former quantity is straightforwardly related to the cathodic efficiency of the system and process investigated; the second yields information on the anodic kinetics and, in particular, on the interaction of JGB with the Cu electrodeposit under anodic polarisation. These two quantities are reported as a function of rotation rate in Figures 6 and 7.

From Figure 6 it can be noticed that: (i) a parabolic, Levich-type dependence is found of the integrated charge on the rotation rate, (ii) the differences found between the two baths are coherent with those found in the i_L plots. This result therefore indirectly confirms our i_L data.

In Figure 7 the stripping curves are not measurably shifted in the presence of JGB, indicating that JGB exhibits no anodic inhibiting effects, probably owing to anodic desorption of this cationic species.

3.2. *In situ surface enhanced raman spectroscopy (SERS)*

3.2.1. *Potential-dependent SERS measurements*

A metallographically polished Cu electrode, immersed in the relevant electrodeposition bath exhibits an OCV of 0.011 ± 0.007 V. This electrode was polarised at −0.1 V for 1 min before acquiring the SERS spectra. A typical spectrum is shown in Figure 8; the corre-

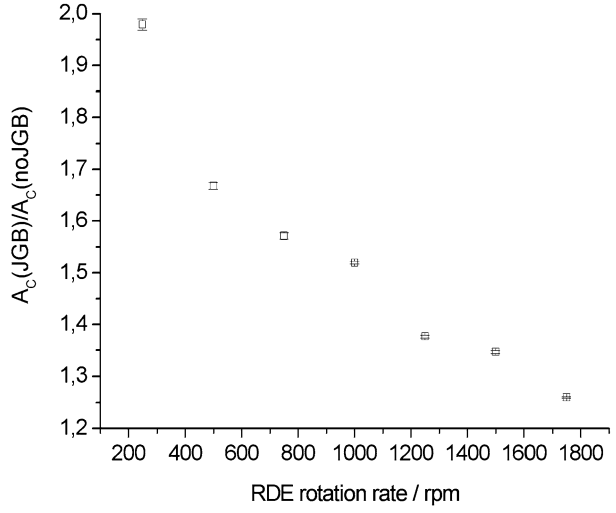

Fig. 5. Ratio of the charges consumed during the cathodic portions of the scans in JGB-containing (A_C(JGB)) and JGB-free (A_C(noJGB)) baths as a function of RDE rotation rate and bath chemistry.

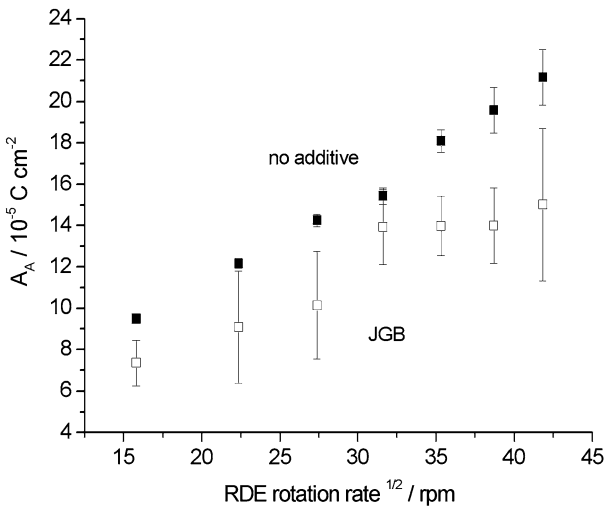

Fig. 6. Integrated charge A_A consumed under the voltammetric anodic stripping peaks, as a function of RDE rotation rate and bath chemistry.

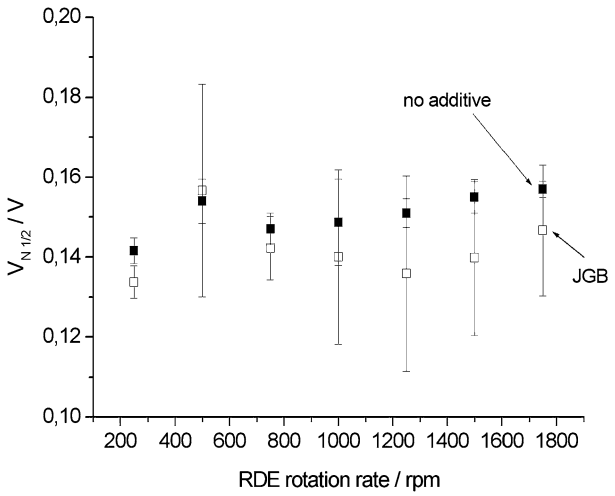

Fig. 7. Half-wave potential $V_{N1/2}$ of the voltammetric anodic stripping peaks, as a function of RDE rotation rate and bath chemistry.

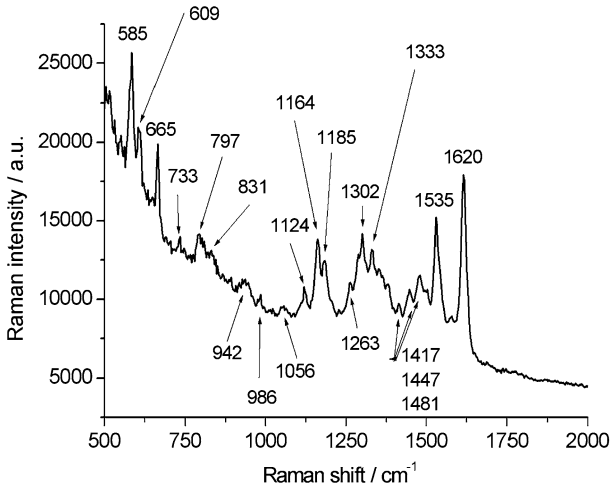

Fig. 8. In situ SERS spectrum measured during Cu potentiostatic electrodeposition at −0.2 V, from the JGB-containing bath with indication of the chief bands (see Table 1).

sponding band assignment is proposed in Table 1. The SERS acquisition spectra sequence was the following: the potential was stepped with an interval of 0.1 V in the cathodic direction up to −0.8 V, then it was stepped from −0.8 to 0.05 V, thus reaching the anodic range, and finally stepped in the anodic direction at the following potentials: 0.1, 0.2, 0.3 and 0.4 V. The potential-dependent spectra are better displayed by grouping the potentials in the following polarisation ranges: low cathodic (Figure 9), high cathodic (Figure 10) and anodic (Figure 11). SERS spectra can be easily observed at intermediate polarisation, while at high cathodic and anodic potentials bands related to the presence of JGB are lost. No measurable changes in spectral patterns are found across the potential range investigated, even though the relative intensities of the different bands change in a subtle way; this behaviour is indicative of the fact that changes in the vibrational characteristics of the adsorbed moieties due to reaction or major reorientation of the molecule can be detected at the electrode, under the conditions studied. Of course, the details of the intensity variations may relate to the reorientation of particular moieties of the molecule, but this analysis is beyond the scope of the present paper.

In Figure 9 we show SERS bands corresponding to low cathodic polarisation: −0.1 to −0.4 V. In this system SERS activity is achieved after ca. 1 min and it is much more straightforward to record SERS spectral than in PEG [8, 9] and SPS [10] containing acidic sulphate Cu plating baths. The SERS activity is essentially the same in the range −0.1 to −0.3 V, but it decreases at −0.4 V, probably owing to changes in the electrocrystallisation

Table 1. List of the chief SERS bands of JGB at a Cu electrode and corresponding assignments

Band position/cm^{-1}	Band assignment	Ref. [19]
585	Heteroaromatic condensed ring vibrations	p. 400 + phenazine
609	idem	
665	Aromatic CH stretching	p. 400
733	Heteroaromatic condensed ring vibrations	Phenazine
797	Aromatic CH wag	p. 279
831	Idem	
942	Olefinic CH wag	pp. 249, 399
986	Idem	
1056	Idem	
1124	Heteroaromatic condensed ring vibrations	p. 400 + phenazine
1164	Idem	
1185	Idem	
1263	Phenyl C–N stretching	pp. 341, 402
1302	Idem	
1333	Idem	
1417	Semicircle stretching of aromatic ring	p. 267
1447	Idem	
1481	Idem	
1535	N = N stretching	pp. 350–352
1620	Quadrant stretching of substitued benzene ring	p. 264

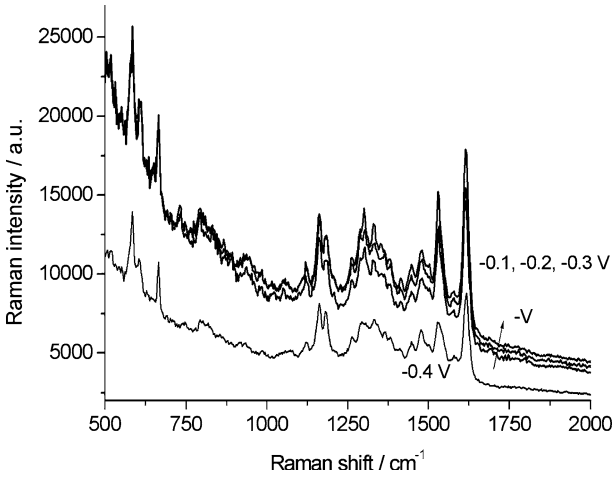

Fig. 9. In situ SERS spectra measured during potentiostatic Cu electrodeposition from the JGB-containing bath: low cathodic polarisations.

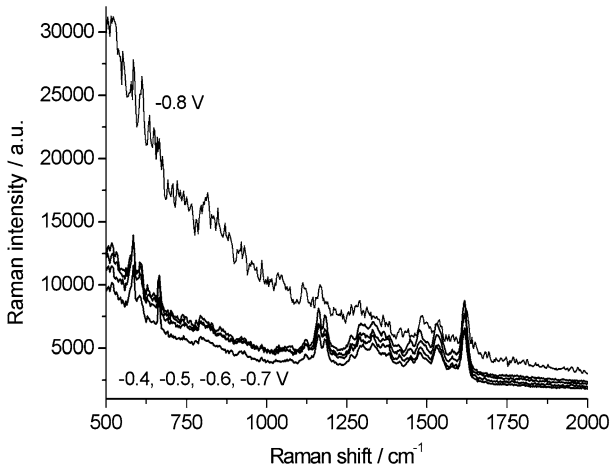

Fig. 10. In situ SERS spectra measured during Cu potentiostatic electrodeposition from the JGB-containing bath: high cathodic polarisations.

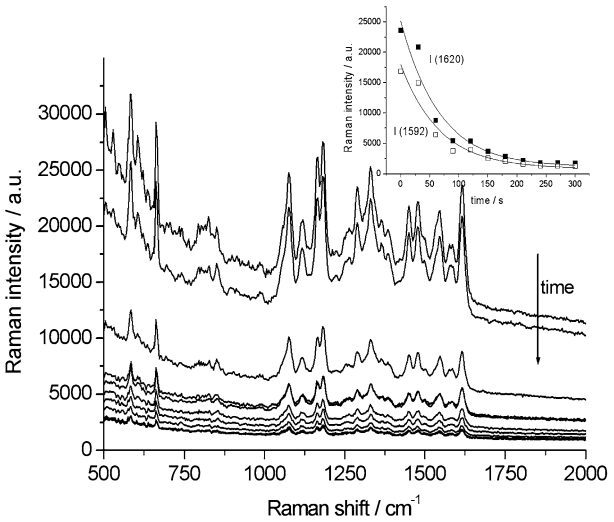

Fig. 12. Time-dependent *in situ* SERS spectra measured during potentiostatic Cu electrodeposition from the JGB-containing bath: potential stepped from −0.8 V to open-circuit. Inset: time-dependent intensities of the bands at 1592 and 1620 cm^{-1}.

mode. The SERS spectra measured at higher cathodic polarisations (−0.4 to −0.8 V) are shown in Figure 10. The quality of the spectra is basically constant up to −0.6 V, it starts to drop at −0.7 V and it decreases dramatically at −0.8 V: this effect is probably due to cathodic desorption from the dynamic electrodic surface rather than to the formation of a non-SERS active surface, because if the polarisation is switched to 0.05 V (Figure 11) or to OC (Figure 12), good-quality spectra are immediately recovered.

In Figure 11 we report the spectra measured in the anodic range (potentials in the range 0.05–0.4 V). A systematic decrease of the spectra quality can be noticed until the JGB features are essentially lost for potentials more anodic than 0.2 V. This degradation of the spectra is probably due to anodic desorption rather than to loss of SERS effect, because if the potential is switched to 0.05 V after polarisation at 0.4 V, a good spectrum is immediately recovered, even though the intensity is somewhat reduced (Figure 13). It is worth noting that at 0.05 V the Cu deposit is anodic and no fresh metal is deposited, thus the surface morphology can the assumed to be unaltered while switching the potential from 0.4 to 0.05 V.

SERS spectra can be also acquired under galvanostatic conditions but we did not investigate this mode of electrodeposition in detail. Preliminary data are reported in Figure 14; the corresponding potentials are reported in Figure 15. Comparison of these data with the respective CV shows that a higher cathodic Tafel slope is required to follow the steady-state data, probably owing to cathodic filming effects. The c.d. at −0.8 V probably contains contributions from JGB reduction and HER. Under similar potential conditions the quality of the galvanostatic spectra is typically lower than that of the potentiostatic ones; a remarkable increase of spectrum quality is observed when depositing at −40 mA cm^{-2}. These differences in SERS behaviour

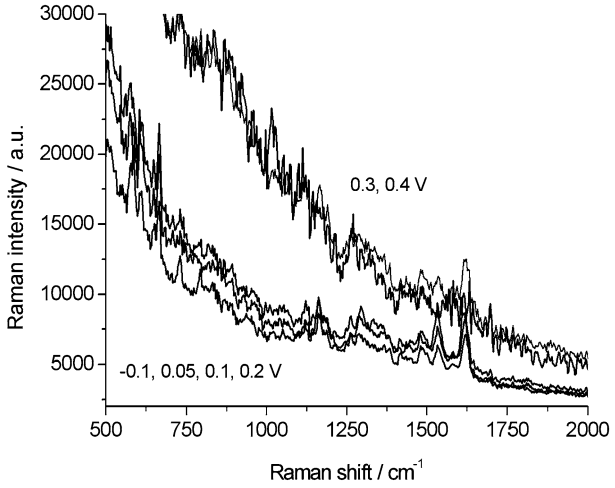

Fig. 11. In situ SERS spectrum measured in the JGB-containing Cu electrodeposition bath: anodic polarisations.

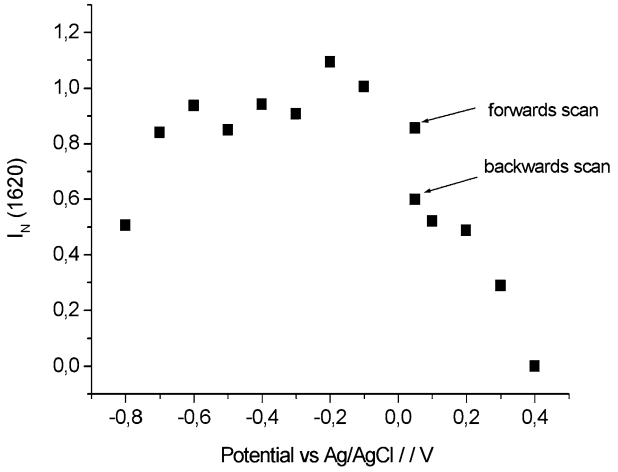

Fig. 13. Normalised Raman intensities derived from *in situ* SERS spectra during potentiostatic Cu electrodeposition in the presence of JGB.

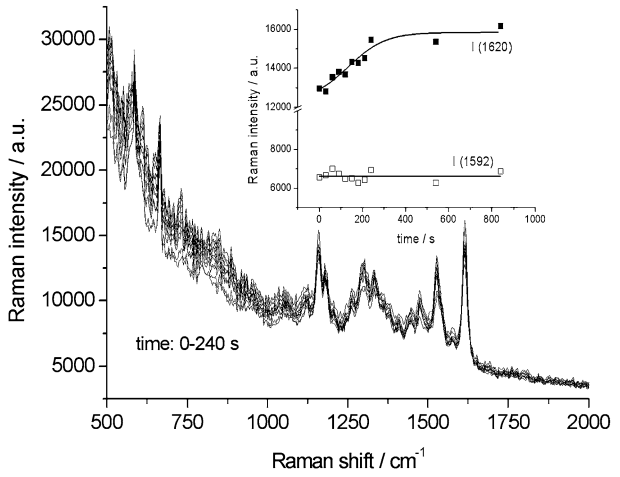

Fig. 14. Time-dependent *in situ* SERS spectra measured during potentiostatic Cu electrodeposition from the JGB-containing bath: potential stepped from −0.8 to −0.2 V. Inset: time-dependent intensities of the bands at 1592 and 1620 cm^{-1}.

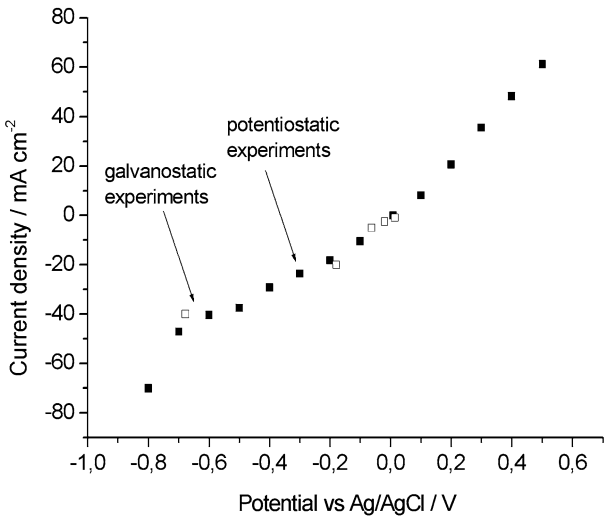

Fig. 16. Current–voltage dependence recorded during potentiostatic and galvanostatic SERS measurements.

between potentiostatic and galvanostatic growth highlight variations of the electrocrystallisation mode and hence of the SERS effect (Figure 16).

In order to account for the potential-dependence of the intensities of the SERS bands, we report the normalised intensity of the band around 1620 cm^{-1} $I_N(1620)$ as a function of potential in Figure 13. $I_N(1620)$ is computed as $I_N(1620) = [I(1620) - I(1592)]/I(1592)$, where $I(x)$ represents the intensity of the raw spectrum at Raman shift x and 1592 cm^{-1} is the position of the first minimum close to 1620 cm^{-1}, taken as a reliable position for the evaluation of the background. Since the background depends on the SERS effect, I_N can be regarded as an estimate of the surface coverage with the relevant adsorbate [9].

Some degree of Stark tuning in the cathodic range can be noticed for bands located around 1535 and 1619 cm^{-1}, that are better resolved probably owing to the fact that they exhibit an orientation better compliant with surface selection rules. The Stark tuning of these bands amounts to -8.3 ± 0.4 and -6.4 ± 0.5 cm^{-1} V^{-1}, respectively. The corresponding linear correlation coefficients ρ^2 are 0.990 and 0.975, denoting a good linearity of the potential dependence. Negative Stark tuning is known in certain instances of chemisorption [20]; a physical interpretation requires understanding of the electrode–molecule bonding which is beyond the scope of this paper.

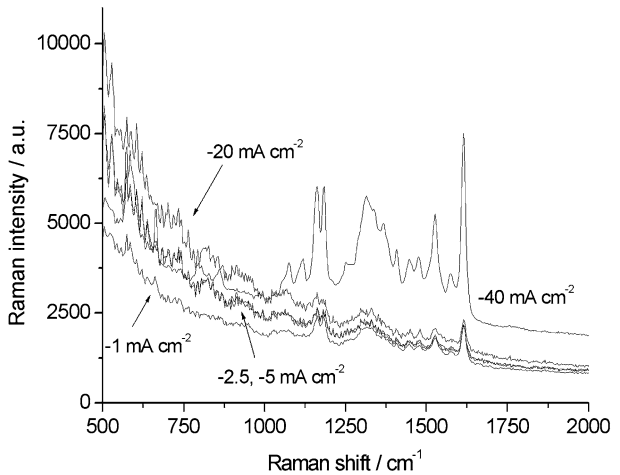

Fig. 15. *In situ* SERS spectra measured in the JGB-containing Cu electrodeposition bath: galvanostatic measurements.

3.2.2. *Time-dependent SERS measurements*

We measured time-dependent SERS spectra in two particular electrodic conditions, in order to assess the development of surface coverage and electrode morphology, related to the degree of surface enhancement. In the first time-dependent experiment we polarised the

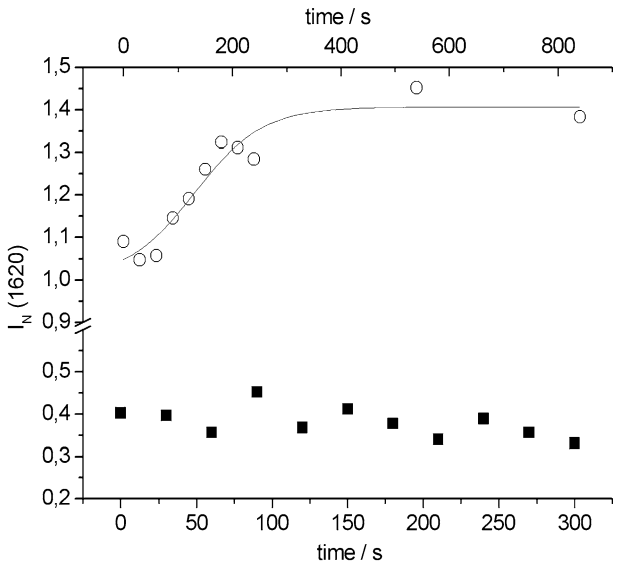

Fig. 17. Time-dependent normalised intensities of the band at 1620 cm^{-1} $I_N(1620)$ derived from *in situ* SERS spectra measured after the potential is stepped from −0.8 V to open circuit (black squares) and from −0.8 to −0.2 V (white circles).

electrode at −0.8 V for 5 min. In these condition the electrodeposition process occurs at a high rate, together with hydrogen evolution. The cell circuit was subsequently interrupted and SERS spectra were recorded during the OC potential decay (Figure 12). In the second time-dependent experiment, after 5 min at −0.8 V, the potential was switched to −0.2 V and SERS were recorded. At −0.2 V electrodeposition proceeds at a lower rate, in the absence of hydrogen evolution (Figure 13).

The time-evolution of the spectra and of the intensities (I(1620), I(1592) and I_N(1620)) are reported in the inset of Figure 12 and in Figure 17 for experiments with final potential at OC and in the inset of Figure 14 and in Figure 17 for experiments with final potential at −0.2 V.

Figures 12 and 14 show that good quality spectra are recovered during the time of the first spectral acquisition after switching the potential from −0.8 V (see Figure 10) to higher potentials. This suggests that SERS active sites are not destroyed at high cathodic polarisations in this system. At OC I(1620) and I(1592) both tend to decrease exponentially with a time constant of ca. 60 s, while I_N(1620) exhibits a very slow decrease (Figure 17). This indicates that in these conditions the surface coverage is essentially constant, while the SERS activity decreases, probably owing to the fact that metal deposition is stopped and the active sites loose their activity in time.

At −0.2 V a different time-dependence is found (Inset of Figure 14 and Figure 17); the Boltzmann curve fits may have a physical meaning in terms of temporal growth of surface coverage, but are essentially meant as guides for the eye). The intensity of the spectra is basically constant, a more detailed analysis shows that I(1592), and hence the SERS activity, is effectively constant, while I(1620), and hence I_N(1620) tend to increase. This behaviour can be interpreted as an increase in surface coverage with adsorbed JGB from −0.8 to −0.2 V, tending towards an asymptotic value. We also tried to record normal-Raman spectra of JGB powder and concentrated solutions but this proved impossible owing to high fluorescence. It can be concluded that Raman work with JGB is possible only in the SERS mode where florescence is quenched.

4. Conclusions

We investigated the behaviour of JGB as the sole additive in acidic sulphate Cu electrodeposition baths. This study is based on cyclic voltammetry performed with an RDE and *in situ* Raman spectroscopy.

From cyclic voltammetry higher nucleation overpotentials are found in the presence of JGB, related to the adsorption of the organic. JGB also causes an increase in the nucleation rate. JGB increases the exchange current density and decreases the cathodic Tafel slope, indicating a variation in the Cu^{2+}-reduction mechanism with respect to the additive-free system. A higher effective diffusion coefficient of Cu^{2+} was measured in the JGB-containing bath. The cathodic reactivity of JGB was highlighted.

Good SERS spectra can be measured in the potential range 0.2 to −0.7 V, encompassing both the anodic and cathodic regimes. No major changes in spectral pattern are found upon varying the potential, nevertheless the surface coverage with the organic and the degree of surface enhancement vary with the electrochemical conditions. The entity of the SERS effect has been followed as a function of potential and time.

Acknowledgments

Highly qualified and continuous technical assistance with all the experiments described in this paper is kindly acknowledged to Francesco Bogani, Dipartimento di Ingegneria dell'Innovazione, Università di Lecce, Italy.

References

1. J.J. Kelly, C. Tian and A.C. West, *J. Electrochem. Soc.* **146** (1999) 2540.
2. J.J. Kelly and A.C. West, *Electrochem. Solid-State Lett.* **2** (1999) 561.
3. K. Kondo, K. Hayashi, Z. Tanaka and N. Yamakawa, *in* P.C. Andricacos, J.L. Stickney, P.C. Searson, C. Reidsema-Simson and G.M. Oleszek (Eds.), ‚Electrochemiocal Processing in ULSI Fabrication III', Vol. 8 (ECS Proc., 2000), p. 76.
4. P. Freundlich, M. Militzer and D. Bizzotto. *in* G.S. Mathad (Ed.), ‚Copper Interconnects, New Contact Metallurgies, Structures, and Low-k Interlevel Dielectrics', Vol. 22 (ECS Proc., 2002), p. 76.
5. S. Miura, K. Oyamada, S. Watanabe, M. Sugimoto, H. Kouzai and H. Honma. *in* G.S. Mathad (Ed.), ‚Copper Interconnects, New Contact Metallurgies, Structures, and Low-k Interlevel Dielectrics', Vol. 22 (ECS Proc., 2002), p. 22.
6. K. Kondo, N. Yamakawa, Z. Tanaka and K. Hayashi, *J. Electroanal. Chem.* **559** (2003) 137.
7. S. Miura and H. Honma, *Surf. Coat. Technol.* **91** (2003) 169–170.
8. B. Bozzini, C. Mele, L. D'Urzo, G. Giovannelli and S. Natali, *J. Appl. Electrochem.* (in press).
9. B. Bozzini, C. Mele and L. D'Urzo, *J. Appl. Electrochem.* **36** (2006, in press).
10. B. Bozzini, L. D'Urzo, C. Mele and V. Romanello, *Trans. Inst. Metal Finish.* accepted.
11. F. Texier, L. Servant, J.L. Bruneel and F. Argoul, *J. Electroanal. Chem.* **446** (1998) 189.
12. J.P. Healy, D. Pletcher and M. Goodenough, *J. Electroanal. Chem.* **338** (1992) 167.
13. E. Gileadi, *Electrode Kinetics* (VCH Publishers Inc., NY, 1993), pp. 87.
14. E.E. Farndon, F.C. Walsh and S.A. Campbell, *J. Appl. Electrochem.* **25** (1995) 574.
15. G.-S. Tzeng, *Plat. Surf. Fin.* (1995) 67.
16. J.J. Kelly and A.C. West, *J. Electrochem. Soc.* **145** (1998) 3472.
17. A.R. Despic. *in* B.E. Conway, J.O'M. Bockris, E. Yeager, S.U.M. Khan, R.E. White (Eds.), ‚Comprehensive Treatise of Electrochemistry', Vol. 7 (Plenum Press, N.Y., 1983), p. 451.
18. W. Plieth, *Electrochim. Acta* **37** (1992) 2115.
19. N.B. Colthup, L.H. Daly and S.E. Wiberley, *Introduction to Infrared and Raman Spectroscopy* (Academic Press, Boston, 1990).
20. S.A. Wasileski and M.J. Weaver, *Faraday Disc* **121** (2002) 285.